Magnetic flux sheets and bubbles:

Investigating extended granular-sized magnetic flux emergence in the quiet Sun

SAIDA MILENA DÍAZ CASTILLO[1,2], CATHERINE FISCHER[3], FERNANDO MORENO-INSERTIS[4,5], SALVATORE GUGLIELMINO[6]
RYOKO ISHIKAWA[7], SERENA CRISCUOLI[8]
1. French-Spanish Laboratory for Astrophysics in the Canaries (FSLAC), 2. Institut für Sonnenphysik (KIS), 3. European Space Agency (ESA) 4. Instituto de Astrofísica de Canarias (IAC), 5. Universidad de La Laguna, 6. INAF - Catania Astrophysical Observatory, 7. National Astronomical Observatory of Japan, 8. National Solar Observatory (NSO)

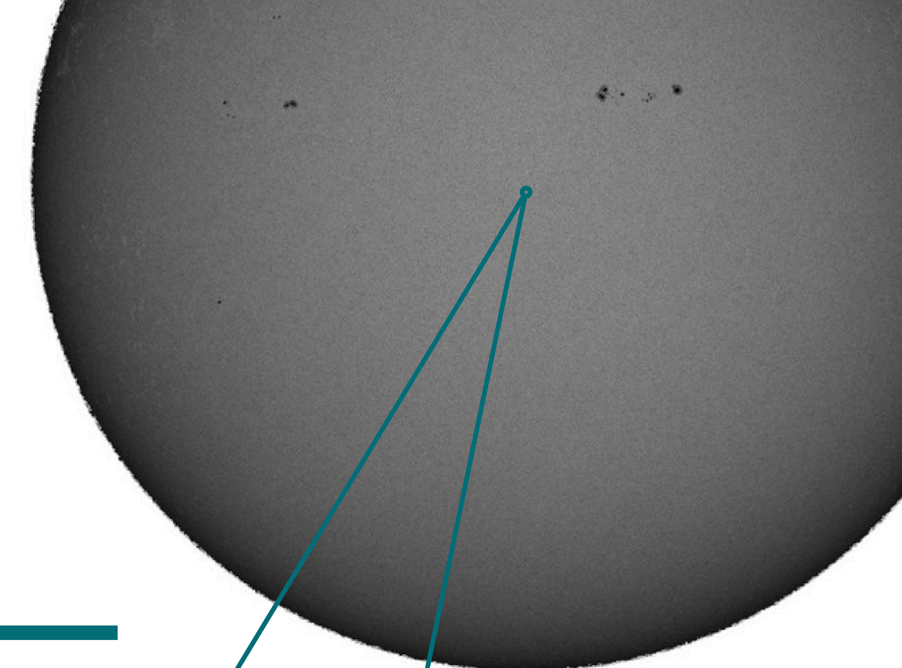

INTRODUCTION

Magnetic flux emergence is a pervasive process across the solar atmosphere at several spatial and temporal scales. Particularly, **small-scale magnetic flux emergence** in the quiet Sun is crucial for maintaining solar magnetic activity. At such scales, **convective plasma flows** driving photospheric granulation are central to turbulent magneto-convection. These flows transport internal magnetic flux upward through an advective-diffusive regime, leading to nonlinear **plasma-magnetic field interactions**. Within individual granules, two primary mechanisms have been identified:

1. Magnetic loops — (Martínez-González and Bellot Rubio, 2009): Bipolar, sub-granular magnetic loops, which maintain their structural coherence. These are transported to the solar surface at the edges of the granules.

2. Magnetic flux sheets — (Moreno-Insertis et al. 2018 and Fischer et al. 2019): Bipolar, extended magnetic configuration emerging within granules and characterised by **an organised and expanding horizontal magnetic field component.**

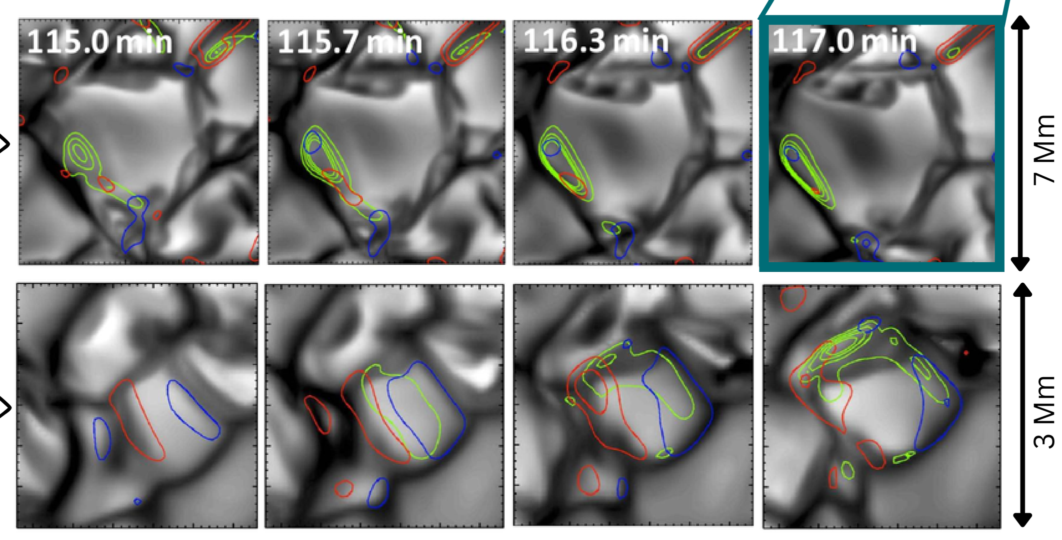

Fig. 1: Bifrost numerical simulations from Moreno-Insertis et al. 2018. Time series of the polarisation isocontours: Total circular (red and blue) and linear (green) polarisation. Background: Continuum intensity.

We investigate granular-sized magnetic flux sheets, inferring their frequency on the solar surface and their contribution to the photospheric magnetic budget. In addition, we study the plasma dynamics and granular-scale phenomena associated with their emergence, alongside their chromospheric counterparts: magnetic bubbles.

DATA AND METHODS

- **Photospheric and Chromospheric observations:**
  - Hinode Spectropolarimeter (SP): 2007 - 2008, and Swedish Solar Telescope (SST) CRISP, 2011 and 2019.
  - Full spectropolarimetry of Fe I lines at 630.1 nm, 630.2 nm and 617.3 nm.
  - Total of ~25 hours with an overall FOV ~40 Mm^2
  - CRISP instrument with full Spectropolarimetry at the Ca II line at 854.2 nm.
- **Magnetic flux sheet detection:**
  - Simultaneous evolution of a horizontal magnetic flux patch with a co-located host granule.
  - Host granule identification: Nearby regions of positive horizontal flow divergence (*DeepVel* Asensio Ramos et al. 2017) and with a generalised upward flow field (Bisector velocity).
- **Characterisation and physical parameters:**
  - The vertical and horizontal components of the magnetic field give the magnetic configuration of the magnetic flux sheet.
  - Horizontal velocity field and its divergence allow us to identify the host granule.
  - Vertical velocity field allow us identify ascending flows.

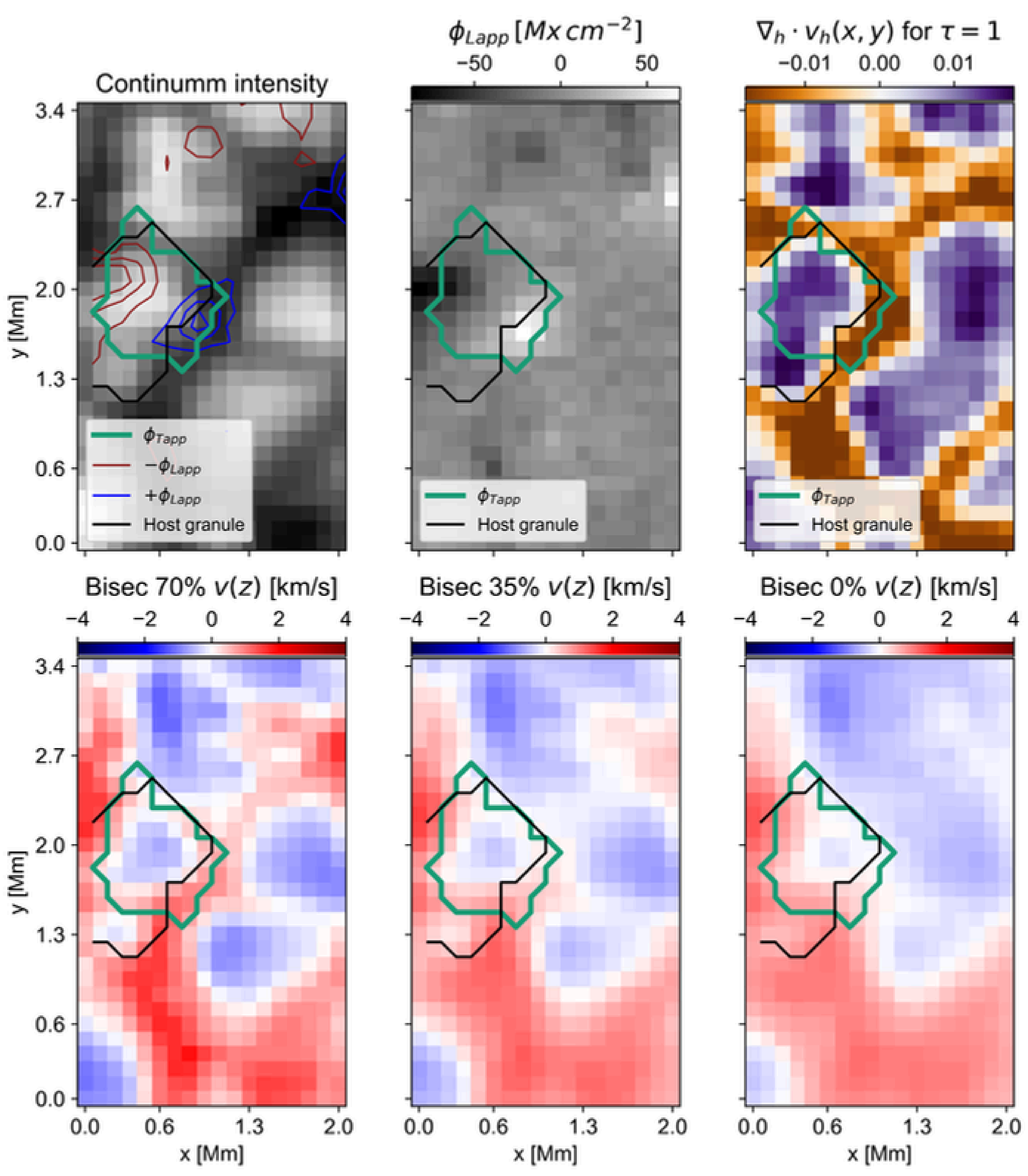

Fig. 2: Magnetic flux sheet event recorded by Hinode SP on September 26 2007, at 08:15UT. 1) continuum intensity in the background with contours. 2) Pine green countours mark a threshold of 130 Gauss for the apparent horizontal magnetic flux density patch $B_{x,y}$. The blue (red) contours mark positive (negative) polarity of the vertical magnetic flux density $+B_z$ ($-B_z$) with thresholds of 20, 40 and 60 Gauss. The black contours mark the boundary of the host granule defined by a single closed contour of zero-divergence. 3) Divergence of the apparent horizontal velocity field marking the horizontal magnetic flux density patch (pine green contour) and the boundary of the host granule (black contour). 4) Bisector velocity field for the three different depth positions: 70%, 35%, and core (0%) of the Fe I 630.15 nm line, corresponding roughly to the low, middle, and high photosphere, respectively. Adapted from Diaz-Castillo et al. 2025.

MAGNETIC FLUX SHEETS: STATISTIC

Description and properties of the events :

- Confirmation of 42 events in the dataset.
- Lifetimes ranging from 3 to 10 minutes and sizes from 0.25 to 1 Mm^2.
- In all cases, the ascending and expanding horizontal magnetic field component evolves together with the host granule.

Magnetic flux sheets have different properties compared to magnetic loops:

	Magnetic flux sheets	Magnetic loops
Occurence rate	0.27 per day and Mm^2	1 per day and Mm
Average unsigned magnetic flux contribution per event	1.6×10^{17} Mx	0.9×10^{17} Mx
Average unsigned magnetic flux over the solar surface per day	0.3×10^{24} Mx	1.1×10^{24} Mx

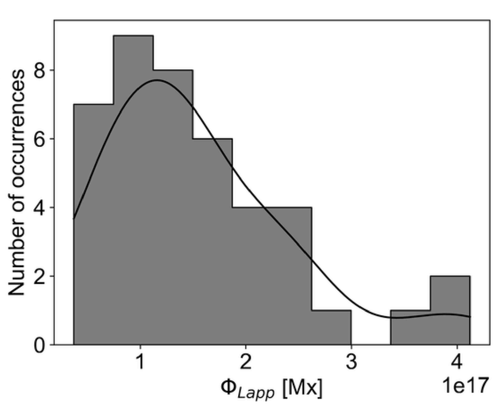

Fig. 3: Total longitudinal magnetic flux measured in the footpoints of the magnetic flux sheet events. The histogram includes the kernel density estimate (KDE). From Díaz-Castillo et al. 2025

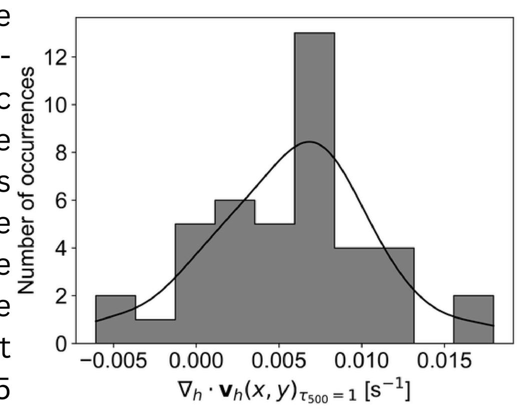

Fig. 4: Divergence of the horizontal plasma flow co-located with the magnetic flux sheet area. The horizontal velocity flow is estimated at τ = 1. The histogram includes the kernel density estimate (KDE). From Díaz-Castillo et al. 2025

Magnetic flux sheet emergence is associated with diverse granules:

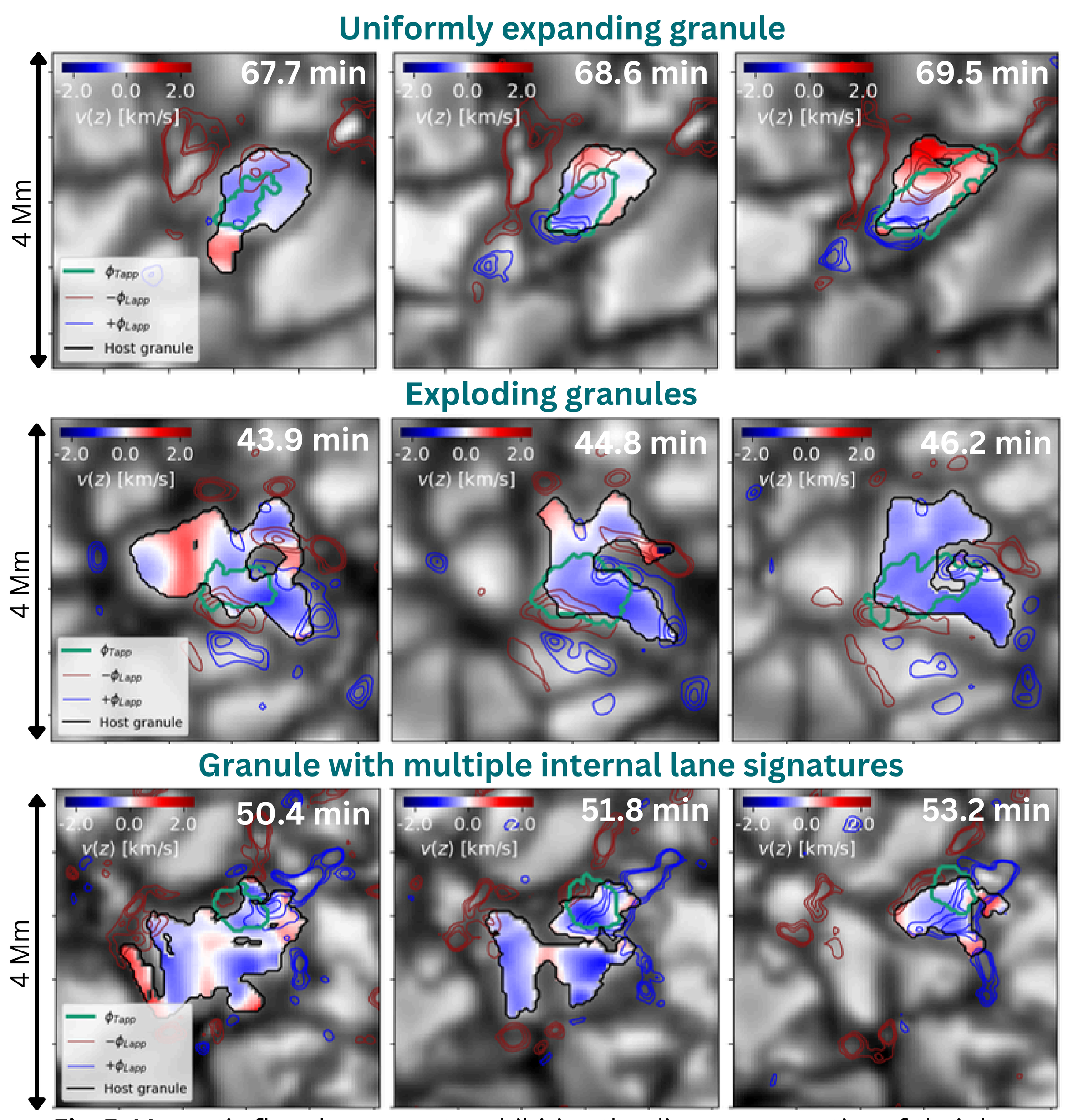

Fig. 5: Magnetic flux sheet events exhibiting the diverse properties of their host granules. Continuum intensity in the background. Pine green contours mark a threshold of $5 \times 10^{-3}\ I_c$ for the total linear polarisation degree. The blue (red) contours mark the positive (negative) polarity of the vertical magnetic flux density with thresholds of 40, 60 and 80 Gauss. The black contours mark the boundary of the host granule. Colour maps within the host granule show the distribution of the bisector velocity at 60% of the line depth. Adapted from Díaz-Castillo et al. 2025.

MAGNETIC BUBBLE: EVIDENCE

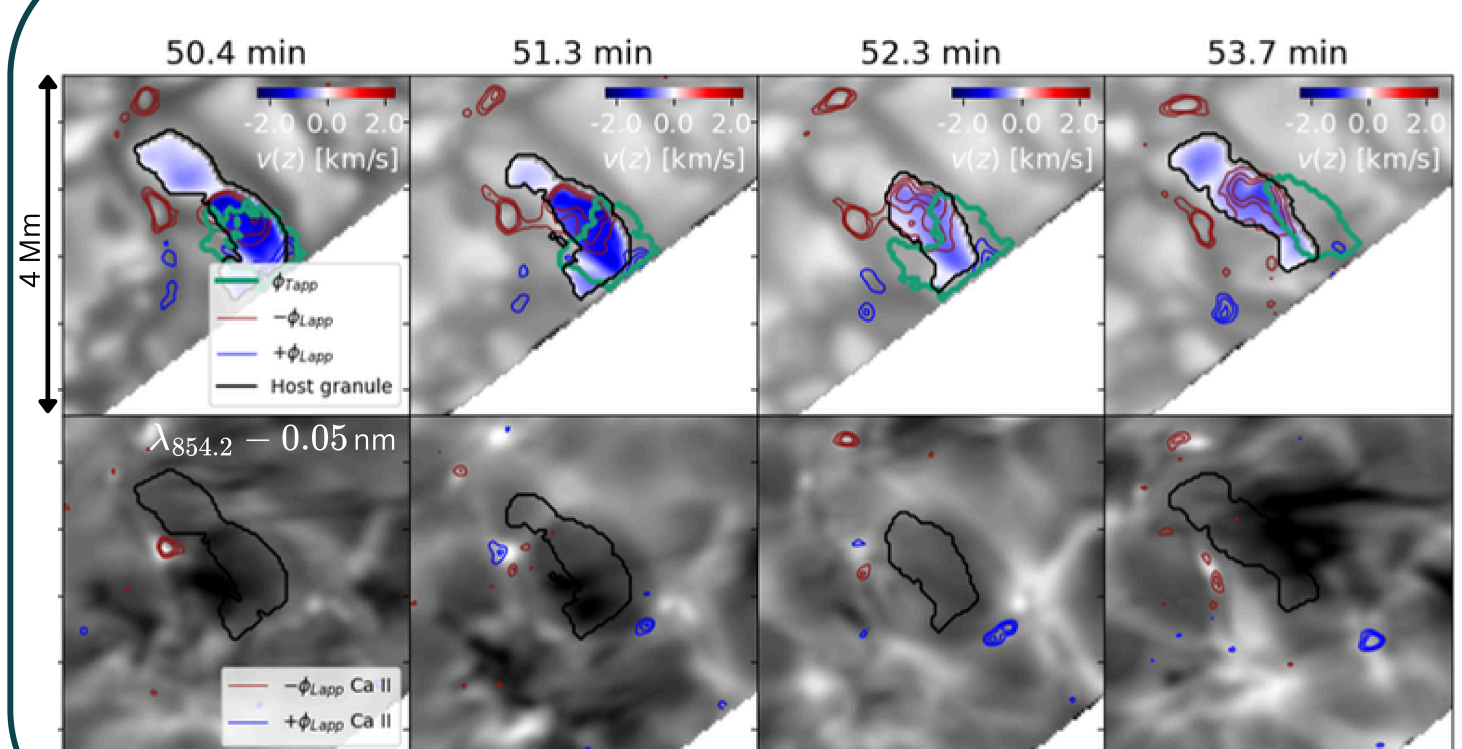

As defined by Ortiz et al. (2014), magnetic bubbles are three-dimensional (3D) semi-spherical structures at chromospheric heights, characterised by a dark-blob signature in filtergrams taken in the wings of the Ca II 854.2 nm line. Using numerical simulations of the chromosphere, a rising magnetic flux structure produces a large, cool, magnetised bubble.

Fig. 6: Magnetic flux sheet event exhibiting a magnetic bubble in the chromosphere. Upper: Same configuration and parameters as Fig. 4. Lower: Filtergrams at the blue wing of the Ca II line at 854.2 nm. The blue (red) contours mark the positive (negative) polarity of the vertical magnetic flux density with thresholds of 30, 40 and 50 Gauss inferred by WFA of the polarisation signal of the Ca II.

SUMMARY AND DISCUSSION

Using spectro-polarimetric information of photospheric iron lines, we developed a two-step method to identify **magnetic flux sheet emergence events**: detecting magnetic flux patches based on the calculation of **the transverse and longitudinal magnetic flux densities, and associating them with their host granules using velocity field analysis**. We confirm 42 events as true identifications.

- Magnetic flux sheets contribute to the small-scale magnetic flux budget with an average of **0.3 x 10^{24} Mx per day** (~30% of the total absolute vertical magnetic flux of the quiet surface (Gošić et al. 2014)).
- Those have an **occurrence rate of 0.27 events per day and Mm^2**, in agreement with simulations (Moreno-Insertis et al. 2018) and **emerge in association with ascending and divergent granular flows**.
- **Magnetic flux sheets emerge in association with a variety of granular phenomena**, which could indicate the potential role of shallowed and recycled magnetic flux in facilitating flux sheet emergence.
- Host granules of magnetic flux sheets with particularly **large upflow velocities can promote the formation of magnetic bubbles associated with the magnetic flux emergence**. An a extenderd stadistical study of such events in the quiet Sun is need to stablish the occurence rate of magnetic bubbles.

References:

- Asensio Ramos, A., Requerey, I. S., & Vitas, N. 2017, A&A, 604, A11.
- Fischer, C. E., Borrero, J. M., Bello González, N., & Kaithakkal, A. J. 2019, A&A, 622, L12.
- Gošić, M., Bellot Rubio, L. R., Orozco Suárez, D., Katsukawa, Y., & del Toro Iniesta, J. C. 2014, ApJ, 797, 49.
- Martínez González, M. J. & Bellot Rubio, L. R. 2009, ApJ, 700, 1391
- Moreno-Insertis, F., Martinez-Sykora, J., Hansteen, V. H., & Muñoz, D. 2018, ApJ, 859, L26
- Ortiz A., Bellot Rubio, L. R, Hansteen V. H., de La Cruz Rodríguez, J & van der Voort, L.R. 2014, ApJ, 781, 126

Results presented here are published in Díaz-Castillo et al. *Astronomy & Astrophysics* 695, A45 (2025)

Nº 30